Draft version October 15, 2026
Typeset using LaTeX **twocolumn** style in AASTeX7.0.2

arXiv:2610.18968v1 [astro-ph.GA] 13 Oct 2026

The Dance of the Little Red Dots: Spectroscopy of Two Blue Companions at $z = 3.9$ and 5.5 Reveals Young, Metal-Poor Starbursts Merging with Their LRDs within a Few Hundred Myr

Fabio Pacucci [1] and Pierluigi Rinaldi [2,3]

[1] *Center for Astrophysics | Harvard & Smithsonian, 60 Garden St, Cambridge, MA 02138, USA*
[2] *Department of Astronomy, University of Texas, Austin, TX 78712, USA*
[3] *Cosmic Frontier Center, The University of Texas at Austin, Austin, TX 78712, USA*

ABSTRACT

The Little Red Dots (LRDs) are compact, red sources, abundant at $4 \lesssim z \lesssim 9$ and likely powered by massive black holes. Photometric studies have found blue companions around them, but none has yet been confirmed spectroscopically. This Letter presents the only two LRD–companion pairs with spectroscopy of both members in the literature: "Waltz" at $z = 3.9$ and "Tango" at $z = 5.5$, with projected separations of 3.6 and 2.5 kpc. Both companions lie at the redshift of their LRD, within $132\,\mathrm{km\,s^{-1}}$ and $57\,\mathrm{km\,s^{-1}}$, and are physically identical, but 524 Myr apart: starbursts $\lesssim 50$ Myr old, metal-poor ($0.2\,\mathrm{Z_\odot}$), dust-free, dynamically cold, and as bright as the LRDs themselves in the rest-frame UV. The LRD in Waltz hosts a $\approx 3 \times 10^6\,\mathrm{M_\odot}$ black hole accreting at half the Eddington rate, a factor of a few above the birth mass of a direct collapse black hole, and is embedded in gas as metal-poor as its companion. Orbital modeling shows that Tango is bound in 81% of the allowed orbits and that Waltz is bound if its host halo exceeds $5 \times 10^{10}\,\mathrm{M_\odot}$. Both blue companions then merge with their respective LRD within a few hundred Myr. We conclude that we are observing what heavy seeding requires: a young black hole beside the metal-poor starburst that the synchronized-pair scenario predicts, in the last steps of a cosmic dance that ends in a merger, and in a galaxy seeded by its black hole.

Keywords: Active galaxies (17) — Early universe (435) — Galaxy evolution (594) — Starburst galaxies (1570) — Supermassive black holes (1663) — Surveys (1671)

1. INTRODUCTION

The Little Red Dots (LRDs) are compact, red sources discovered by the *James Webb Space Telescope* (JWST) in its first deep-field campaigns (D. D. Kocevski et al. 2023; Y. Harikane et al. 2023; J. Matthee et al. 2024; R. Maiolino et al. 2024). Photometric censuses now count hundreds of LRDs over the redshift range $4 \lesssim z \lesssim 9$ (V. Kokorev et al. 2024; D. D. Kocevski et al. 2025; H. B. Akins et al. 2025; P. Rinaldi et al. 2026a), suggesting an average surface density of $\approx 1\,\mathrm{arcmin^{-2}}$ (P. Rinaldi et al. 2026a; P. G. Pérez-González et al. 2026).

Two properties generally define the class: (i) compactness at optical wavelengths (R. E. Hviding et al. 2026; P. Rinaldi et al. 2026a), with typical effective radii of $\lesssim 100$ pc (J. F. W. Baggen et al. 2023), and (ii) a V-shaped spectral energy distribution (SED), characterized by a blue UV and a red optical continuum with, on average, a turnover near the Balmer limit (D. J. Setton et al. 2025; D. D. Kocevski et al. 2025).

Spectroscopic data have sharpened the puzzle. Broad Balmer lines, with widths of $1000 - 3000\,\mathrm{km\,s^{-1}}$, are detected in a large fraction of the LRDs observed with NIRSpec (J. E. Greene et al. 2024; M. Killi et al. 2024; A. J. Taylor et al. 2025), and the same spectra frequently show Balmer absorption, which requires dense gas along the line of sight (F. D'Eugenio et al. 2025a; I. Juodžbalis et al. 2026). If those lines are virialized, the implied black hole masses lie $1 - 2$ orders of magnitude above the local expectation for the stellar mass of the host (F. Pacucci et al. 2023; B. L. Jones et al. 2025; A. R. Gupta et al. 2026). However, the X-ray emission such black holes should produce is rarely detected (R. Maiolino et al. 2025; F. Pacucci & R. Narayan 2024; P. Madau & F. Haardt 2024; E. Lambrides et al. 2026). The virial black hole mass estimate is also under scrutiny, since electron scattering in a dense envelope can broaden a narrow line and inflate the inferred mass,

Corresponding author: Fabio Pacucci
Email: fabio.pacucci@cfa.harvard.edu

potentially leading to an overestimate (V. Rusakov et al. 2026; E. Modelevsky et al. 2026).

The most basic question is still unanswered: *what powers an LRD?* Explanations divide on whether an accreting black hole is present at all. For instance, using radiation-hydrodynamic simulations, F. Pacucci et al. (2026) showed that the population's observational signatures follow if LRDs are powered by accreting direct collapse black holes (DCBHs) inside their natal halos. A second interpretation attributes the reddening to gas immediately around the black hole, as in the "black hole star" picture (R. P. Naidu et al. 2026). If no black hole is assumed, the LRD is a different kind of system: a globular cluster in formation (J. Chisholm et al. 2026), a single supermassive star (D. Nandal & A. Loeb 2026), or a cluster powered by repeating tidal disruption events (J. Bellovary 2025). Of these models, direct collapse places demands on an LRD's immediate surroundings.

Direct collapse (A. Loeb & F. A. Rasio 1994; S. P. Oh & Z. Haiman 2002; V. Bromm & A. Loeb 2003; M. C. Begelman et al. 2006; G. Lodato & P. Natarajan 2006) produces seeds with initial masses of $10^4 - 10^6\,M_\odot$ (A. Ferrara et al. 2014). The collapse proceeds only where: (i) the gas is pristine, (ii) the halo has reached the atomic-cooling threshold, and (iii) an external flux of Lyman-Werner (LW) photons ($11.2 - 13.6$ eV; B. T. Draine & F. Bertoldi 1996) dissociates H_2 and suppresses fragmentation (K. Omukai 2001; M. A. Latif et al. 2014; K. Inayoshi et al. 2020). Since the flux falls rapidly with increasing distance, the irradiating source must be a near neighbor.

In the "synchronized pair" scenario, two halos collapse nearly together, and the one that forms stars first irradiates the other (M. Dijkstra et al. 2008; E. Visbal et al. 2014; J. A. Regan et al. 2017). P. Rinaldi et al. (2025) presented the first statistical census of LRD UV morphologies in the JADES fields and found that at least 30% of LRDs have close companions in the rest-frame UV, challenging the initially assumed compact morphology inferred from rest-frame optical observations. Recently, J. F. W. Baggen et al. (2026) and A. J. Barger & L. L. Cowie (2026) reported that compact, UV-bright companions of LRDs lie at projected separations of $0.5 - 5$ kpc; M. Golubchik et al. (2026) also reported a similar case behind a lensing cluster.

However, because standard galaxies also cluster, proximity alone does not imply a causal link. F. Pacucci & C. M. Urry (2026) therefore measured companion statistics for 253 LRDs against > 7000 control galaxies drawn from the same mosaics, matched in redshift, brightness, and compactness. The brightest quartile of that LRD sample hosts blue companions within 2 kpc at a rate exceeding that of the control sample, significant at 3.3σ. Those companions are also overwhelmingly blue, and significantly bluer than the companions of the control galaxies. Hence, that study concluded that the association is physical.

All results mentioned above are based on photometry. Broad-band colors identify a blue, compact neighbor, but they cannot answer the three questions on which the interpretation is based: (i) whether the neighbor lies at the redshift of the LRD, (ii) whether its blue light is starlight, or rather nebular continuum that the LRD itself could power (C.-H. Chen et al. 2025b), or even part of a larger host in which the nucleus sits (P. Rinaldi et al. 2026b), and (iii) whether the two objects are gravitationally bound.

In this Letter, we present the only two LRD–companion pairs in the literature with spectroscopy for both members. In "Waltz" the LRD GS-206858 and its companion GS-206860 sit at $z = 3.936$, separated by 3.57 kpc in projection; in "Tango" the LRD GS-13971 and its companion sit at $z = 5.4816$, separated by 2.54 kpc. We name the systems after the two dances, the closer pair taking the closer dance.

We describe the observations and the measurements in §2, and present our results in §3. In §4, we discuss what these systems imply for the nature of LRDs. Throughout, we adopt the Planck18 cosmology (Planck Collaboration et al. 2020), where $1''$ corresponds to 7.15 and 6.13 proper kpc at $z \approx 3.9$ and $z \approx 5.5$, respectively.

2. DATA AND METHODS

This Section describes the data available for the two systems and the measurements we derive from them. Both pairs lie in GOODS-S and were observed with NIRSpec, one through the micro-shutter assembly (MSA) and the other with the integral field unit (IFU).

2.1. *Data*

"Waltz" is a pair of JADES sources (M. J. Rieke et al. 2023a; F. D'Eugenio et al. 2025b; D. J. Eisenstein et al. 2026). We use the NIRSpec (P. Jakobsen et al. 2022) MSA spectra of its two members from the public JADES DR3 release, retrieved from MAST: for the LRD GS-206858, the prism and the G140M, G235M, and G395M gratings from PID 1180 (observations o026 and o028, ≈ 3.1 ks per grating per observation); for the companion GS-206860, the same four dispersers in PID 1286 and, independently, in PID 1180. The two programs placed their shutters differently (position angles of 207° and 195°, see also Fig. 1). The companion consists of two knots, A and B (§2.2): the PID 1286 slitlet captures the larger fraction of the light of knot A, the line emitter,

but also much of the continuum of knot B, whereas the PID 1180 slitlet captures less light but is dominated by knot A. We adopt PID 1286 for all luminosities. The standard Level-3 pipeline products of PID 1286 (also from MAST) add a G395H spectrum of the companion at $R \approx 2700$.

"Tango" pairs the LRD GS-13971, first identified as such by J. Matthee et al. (2024, 2026) and Y. Ishikawa et al. (2026a), with a blue companion 0.″415 away. We obtain its spectroscopy from the NIRSpec IFU under program GO 5664 (PI: J. Matthee). We use the Level-3 cubes in PRISM/CLEAR ($0.60 - 5.30$ μm, 6.4 ks) and G395H/F290LP ($2.87 - 5.27$ μm, 36.2 ks), both sampled with 0.″1 spaxels through an eight-point cycling dither; the region at full depth spans $2.″8 \times 2.″8$, which entirely contains the pair.

For Tango, we use the 14 NIRCam bands from F090W to F480M, and five ACS and four WFC3 bands from the DAWN JWST Archive mosaics (0.″05 per pixel, see F. Valentino et al. 2023) reduced with GRIZLI (G. Brammer 2023). For Waltz, we use the same 14 NIRCam bands from the JADES mosaics (0.″03 per pixel, see M. J. Rieke et al. 2023b; D. J. Eisenstein et al. 2026).

2.2. *Separating the Pairs*

In Tango, the two sources are separated by only twice the PSF core width, so we must decompose the cube before any measurement. After subtracting a master background built from source-free spaxels, we construct the PSF empirically from the broad Hα wings of the LRD ($400 < |v| < 1200\,\mathrm{km\,s^{-1}}$), which trace the unresolved broad-line region alone, following the established approach for separating quasars from their hosts in IFU data (B. Husemann et al. 2013; M. A. Marshall et al. 2023; R. Decarli et al. 2024). The PSF requires a core of FWHM 0.″181 and a halo of FWHM 0.″507 carrying $\approx$ 39% of the flux. We then fit each wavelength plane within 0.″80 of the pair midpoint with templates for the LRD, the companion, a third field source, and a quadratic background, rescaling the errors to $\chi^2_\nu = 1$ on line-free planes; the template amplitudes as a function of wavelength are the extracted spectra. The two main templates are nearly orthogonal, and the companion receives only $\approx 3.4\%$ of the LRD's broad-line flux. Two checks calibrate the decomposition: $20 \pm 6\%$ of the LRD's wing flux ends up in the background term, so the companion's template fluxes are lower limits at that level; and the F430M excess of the LRD in the NIRCam image, obtained without the cube, matches the total Hα flux of the extracted spectra.

Waltz requires no such treatment, since its two members were observed as separate MSA targets. The structure to be resolved lies inside the companion, which the imaging splits into two knots 0.″23 apart. In the 2D prism spectrum, the emission lines and the UV continuum trace knot A, while the continuum beyond 2.5 μm is displaced by 0.″050 toward knot B. We cannot cleanly separate the two knots at the 0.″24 effective spatial resolution along the slit. Hence, every spectroscopic quantity we quote for Waltz's companion refers to knot A.

2.3. *Emission Lines and Velocity Offsets*

We fit every line as part of a complex, with a local continuum, a single redshift and width shared by the narrow components, and the [N II] doublet fixed at its theoretical ratio of 2.94 (D. E. Osterbrock & G. J. Ferland 2006). All fits use standard least-squares methods from ASTROPY and SCIPY (P. Virtanen et al. 2020; Astropy Collaboration et al. 2022), with uncertainties from a parametric bootstrap (300 refits), and the error arrays rescaled so that $\chi^2_\nu = 1$ away from the lines. Intrinsic widths require care, because the spectral resolution of an MSA spectrum depends on how the source fills the shutter. Therefore, we quote $\sigma_{\rm int}$ between two bracketing line-spread functions, for a uniformly illuminated shutter and for a compact source; the [O III] line of the Waltz LRD, for instance, is unresolved under the first and gives $52\,\mathrm{km\,s^{-1}}$ under the second.

We measure velocity offsets as companion minus LRD from [O III]λ5008, the strongest line in all four sources. Throughout, we label each system by the [O III] redshift of its LRD: $z = 3.9363$ for Waltz (companion at 3.9386) and $z = 5.4816$ for Tango (companion at 5.4804). For Waltz, the two MSA observations of the companion give $+134.0 \pm 4.2$ and $+127.6 \pm 5.5\,\mathrm{km\,s^{-1}}$ against the same LRD spectrum, and we adopt their weighted mean (their difference is a systematic term). For Tango, the offset is measured on the decomposed G395H spectra, and the systematic is half the spread across the template variants of §2.2; the companion's own [O III] and Hα velocities agree to $0.4\,\mathrm{km\,s^{-1}}$.

The same line fitter provides the broad Hα components. For Waltz, we fit one broad Gaussian shared across three independent extractions of the G395M data. For Tango, we fit the decomposed G395H spectrum.

2.4. *Photometry, SED fitting, and Orbits*

We measure photometry identically in both systems. We convolve all bands to the F480M resolution (FWHM 0.″160), and extract fluxes in apertures of radius 0.″25 for the LRDs and 0.″15 for the companions, using a local background annulus. We separate blended components using a matched Gaussian PSF. Total fluxes follow each LRD's growth curve in the long-wavelength bands, with

Table 1. Properties of the two LRD–companion pairs.

	Waltz	**Tango**
	$z = 3.936$	$z = 5.4816$
LRD–Companion Pairs		
Velocity offset, Δv (companion − LRD)	$+131.6 \pm 6$ km s^{-1}	-56.8 ± 5 km s^{-1}
Projected separation	3.57 ± 0.03 kpc	2.54 ± 0.15 kpc
Probability the pair is bound, $P_{\rm bound}$	$0.48^{+0.23}_{-0.30}$	$0.81^{+0.09}_{-0.10}$
Time to merger	457^{+630}_{-243} Myr	129^{+352}_{-96} Myr
Total mass needed within the separation	$> 7.2 \times 10^9$ M$_\odot$	$> 9.5 \times 10^8$ M$_\odot$
Little Red Dots		
Broad Hα FWHM	1169^{+108}_{-88} km s^{-1}	2132 ± 18 km s^{-1}
Broad Hα profile	unabsorbed	absorbed core
Black hole mass, $\log(M_\bullet/\,{\rm M}_\odot)$	6.3–6.6	7.5–7.8
Bolometric luminosity, $L_{\rm bol}$	1.4×10^{44} erg s^{-1}	1.2×10^{45} erg s^{-1}
Eddington ratio, $f_{\rm Edd}$	0.55	0.34
Narrow-line dust attenuation, A_V	$\simeq 0$	$\simeq 0.9$ mag
Narrow-line velocity dispersion, σ	$\lesssim 52$ km s^{-1}	32–54 km s^{-1}
Host stellar mass, $M_\star$	$< 8.0 \times 10^9$ M$_\odot$	$< 8.3 \times 10^9$ M$_\odot$
Blue Companions		
Hα rest-frame equivalent width	800–950 Å	733 ± 80 Å
Dust attenuation, A_V	$\simeq 0$	$\simeq 0$
Gas-phase metallicity	$\simeq 0.2\ Z_\odot$	$\simeq 0.2\ Z_\odot$
Stellar mass, $M_\star$	6.6×10^7 M$_\odot$	1.7×10^8 M$_\odot$
Star formation rate (Hα)	1.2 M$_\odot$ yr^{-1}	2.6 M$_\odot$ yr^{-1}
Growth timescale, $M_\star$/SFR	56 Myr	65 Myr
Velocity dispersion, σ	20–50 km s^{-1}	47–65 km s^{-1}

NOTE—Photometry and spectra for the Waltz companion include light from an older knot 0.23″ away. This light reddens the SED, which an SED fit reads as $A_V \simeq 0.4$ mag, while the grating Balmer decrements of the line-emitting knot are consistent with Case B. The values in the column refer to the line-emitting knot.

an encircled energy of 0.86 ± 0.05 within 0.″30. The two knots of the Waltz companion are 0.″23 apart, so we cannot rule out some mutual contamination in their photometry.

We checked our totals against the DJA catalog (F. Valentino et al. 2023). For the Waltz LRD, the two measurements agree within 2%, while for the Tango LRD within 10%. For the companions, the catalog totals are 1.8× and 2.9× ours, so the pairs require a deblended, PSF-matched scheme.

We derive stellar properties via SED fitting. We first obtain stellar masses from EAZY (version 0.8.7, G. B. Brammer et al. 2008), using a Chabrier initial mass function (G. Chabrier 2003). We run each fit twice: the first run has no redshift constraints and supplies the photometric redshifts used to test the neighbors of the two LRDs, while the second run fixes the pair redshift to obtain the masses. For the companions, template masses carry systematic uncertainties of ≈ 0.3 dex. For the LRDs, the same fitting procedure yields upper limits on the stellar masses, which are degenerate with the AGN contribution (see, e.g., D. D. Kocevski et al. 2025; E. Durodola et al. 2025). For both LRDs, we retrieve upper limits of $M_\star < 8 \times 10^9$ M$_\odot$. These values are consistent with recent literature (e.g., C.-H. Chen et al. 2025a).

As an independent check on the companions, we also used BAGPIPES (A. C. Carnall et al. 2019), with templates from G. Bruzual & S. Charlot (2003), a Kroupa IMF, nebular emission from CLOUDY (C. M. Gunasekera et al. 2025), a non-parametric continuity star formation history (J. Leja et al. 2019), and broad priors on mass, attenuation, and metallicity. The BAGPIPES masses of the two companions, $\log(M_\star/\,{\rm M}_\odot) = 8.0$ and 8.3, agree with the EAZY values, 7.8 and 8.2, within the 0.3 dex template systematic.

Both codes yield low stellar metallicities ($\lesssim 30\%\, Z_\odot$); for Waltz this is an upper limit, since the photometry includes the older knot B. The gas-phase metallicity measured from the emission lines is $\approx 0.2\, Z_\odot$ for both companions (§3.2); we adopt it in the Hα-to-SFR conversion below, with $0.1 - 0.3\, Z_\odot$ as the systematic range.

In both Tango and Waltz, Hα shows large equivalent widths, indicating that the companions are actively forming stars. With the metallicity-dependent conversions, the ratio SFR(Hα)/SFR(UV) is ≈ 1.5 for the Waltz companion and consistent with unity for the Tango companion, whose template Hα flux is a lower limit (§2.2); a ratio above unity indicates a rising star formation rate, as commonly observed at such low stellar masses (e.g., R. Navarro-Carrera et al. 2026). The absolute values depend on the adopted metallicity at the 0.1 dex level (R. L. Theios et al. 2019). Similarly, their inferred star-formation histories from BAGPIPES show a strong upturn over the last 100 Myr. We discuss the implications of these findings in §3.2.

We use a Monte Carlo ensemble of 6000 orbital realizations per system to infer the orbits from r_p and Δv. We assume isotropic orientations for the separation and velocity vectors. The host is an NFW halo (J. F. Navarro et al. 1996) with a log-uniform mass prior ($10^{10} - 10^{11.5}\,\mathrm{M}_\odot$ for Tango, $10^{10} - 3\times10^{11}\,\mathrm{M}_\odot$ for Waltz) in addition to a Hernquist baryonic component (L. Hernquist 1990) with a log-uniform prior from $10^8\,\mathrm{M}_\odot$ to the EAZY ceiling value, so that the orbits do not depend on a specific, measured host stellar mass. The companion receives a subhalo-mass prior capped at half the host mass. We place the LRD at the center of the gravitational potential of the host and treat the companion as the satellite: the $10^6 - 10^8\,\mathrm{M}_\odot$ black hole marks the bottom of the potential well, the extended host light and the [O III] emission are centered on the LRD, and the companion's dispersion of $20 - 65\,\mathrm{km\,s^{-1}}$ caps its own halo near $10^{10}\,\mathrm{M}_\odot$, which is below what binding requires. If both objects were satellites of a larger halo centered elsewhere, the pair would still be bound but would merge more slowly. We integrate each orbital realization with Chandrasekhar dynamical friction (S. Chandrasekhar 1943) and tidal stripping, and record a merger when the separation falls below 500 pc.

3. RESULTS

We present the two pairs, Tango and Waltz, in parallel throughout this Section. Table 1 collects all measured quantities and their uncertainties for both systems, while the main text discusses only the relevant numbers.

3.1. *Two Physically Associated Pairs*

Every claim in this Letter is based on one fact: the two blue sources are neighbors of their LRDs. Figure 1 shows the two systems in the configuration that photometric surveys have reported around bright LRDs (J. F. W. Baggen et al. 2026; A. J. Barger & L. L. Cowie 2026; F. Pacucci & C. M. Urry 2026) but could not spectroscopically confirm. The projected separations are 3.57 ± 0.03 kpc for Waltz and 2.54 ± 0.15 kpc for Tango.

Both companions lie at the redshift of their LRD (Fig. 2). In Waltz, [O III]λ5008 places the companion at $\Delta v = +131.6 \pm 6\,\mathrm{km\,s^{-1}}$, and the two MSA configurations agree within their errors. In Tango, the decomposed cube gives $\Delta v = -56.8 \pm 5\,\mathrm{km\,s^{-1}}$, and the companion's own [O III] and Hα velocities agree to $0.4\,\mathrm{km\,s^{-1}}$. Each companion shows Hβ, [O III], and Hα at a common redshift (Fig. 3).

These velocity offsets are small, well below the threshold of $500\,\mathrm{km\,s^{-1}}$ (E. Ventou et al. 2017; J. M. Helton et al. 2024) for galaxies in the same structure at these redshifts. For Tango, the orbital ensemble of §3.4 places the companion at a three-dimensional speed of $\approx 114\,\mathrm{km\,s^{-1}}$, against a median escape speed of $315\,\mathrm{km\,s^{-1}}$ at its position. Of course, two confirmations cannot settle the question for the population, but they show that the photometric selection in J. F. W. Baggen et al. (2026) recovers physical pairs.

3.2. *Two Identical Companions Half a Gyr Apart*

The second fundamental question is: what is the blue light? Figure 3 (top) shows a first finding: normalized in the rest-UV, the prism spectra of the two companions are indistinguishable, from the Lyman break to Hα and beyond. They share the same flat blue continuum and emission lines with the same relative strengths. Two galaxies separated by 524 Myr of cosmic time, selected only for sitting beside an LRD, are identical: a young starburst caught within its first tens of Myr.

The Hα equivalent widths, $800 - 950$ Å in Waltz and 733 ± 80 Å in Tango, are reached only by a single burst younger than ≈ 6 Myr, or by continuous star formation younger than ≈ 100 Myr (C. Leitherer et al. 1999; J. J. Eldridge et al. 2017). The gas that formed the stars is metal-poor (M. Curti et al. 2020): $12 + \log(\mathrm{O/H}) \simeq 8.0$, i.e., $0.2\, Z_\odot$ in both companions. The same finding is confirmed by the [N II]/Hα ratios, < 0.06 for the Waltz companion (G395H) and 0.053 ± 0.010 for the Tango companion, measured on the decomposed G395H spectrum ($R \approx 2700$), where [N II]λ6583 is ~ 900 km s^{-1} from Hα and fully resolved. The gas is also dust-free, with Balmer decrements consistent with Case B in both systems: 2.53 ± 0.12 for the Tango companion (from

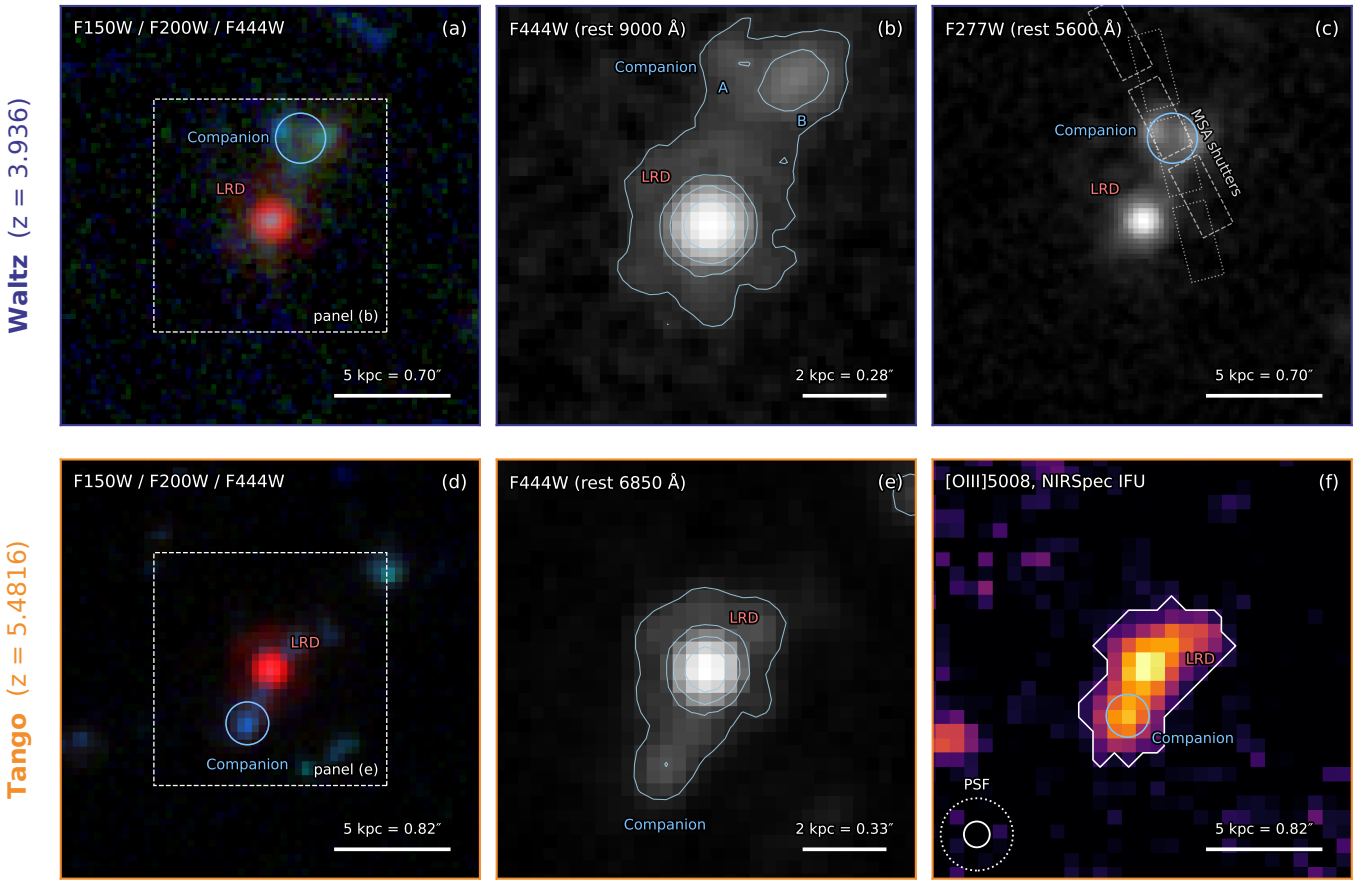


Figure 1. The two LRD–companion pairs. Top row: Waltz ($z = 3.936$). Bottom row: Tango ($z = 5.4816$). *(a), (d):* NIRCam composites of F150W, F200W, and F444W (blue, green, and red channels); the dashed box marks the region shown in the adjacent panel. *(b), (e):* F444W alone, sampling the rest-frame optical, where the LRD dominates. *(c):* F277W, which contains [O III] and Hβ at $z = 3.936$, where the companion is conspicuous; the dashed and dotted rectangles are the open MSA shutters of the two companion observations. *(f):* [O III]λ5008 map from the NIRSpec IFU, integrated around the pair's systemic velocity; the white outline encloses the region where the line is detected, and the companion appears as a distinct peak within it. The projected separations are 3.57 and 2.54 kpc. The concentric circles in the lower left of (f) show the FWHM of the core (0.″18, solid) and halo (0.″51, dotted) of the empirical IFU PSF (§2.2).

its G395H spectrum), where Hβ and Hα are resolved from [O III] and [N II]; 2.8 ± 0.4 and 3.8 ± 0.5 for the Waltz companion in its two grating observations. The gas is cold, with intrinsic dispersions of $20 - 50$ and $47 - 65\,\mathrm{km\,s^{-1}}$.

We also estimate stellar masses of 6.6×10^7 and $1.7 \times 10^8\,\mathrm{M_\odot}$, against star formation rates of 1.2 and $2.6\,\mathrm{M_\odot\,yr^{-1}}$, from the metallicity-dependent Hα conversion of N. A. Korhonen Cuestas et al. (2025) at the measured $Z \simeq 0.2\,Z_\odot$ (adopting 0.1 or $0.3\,Z_\odot$ changes them by ± 0.05 dex): both galaxies assembled most of their stars within the last 100 Myr. Non-parametric star formation histories fitted with BAGPIPES agree: in both companions the star formation rate rises steeply over the last ~ 100 Myr to its present Hα value, while older stars are only loosely constrained. In Waltz, older stars do sit next to the burst: knot B, 0.″23 from the line-emitting knot A, shows a Balmer break between F150W and F182M and has a stellar mass of $4 \times 10^8\,\mathrm{M_\odot}$.

This light belongs to the companion galaxies, not to nebular gas photoionized by the LRD nor to an off-center clump of the LRD's host, the two alternatives that broad-band colors left open (C.-H. Chen et al. 2025a,b; P. Rinaldi et al. 2026b). Three facts exclude them. First, the velocities, as each companion moves at its own systemic velocity, 132 and $57\,\mathrm{km\,s^{-1}}$ away from its LRD, and its lines are narrow; gas merely illuminated by the LRD would move with the LRD. Second, the line ratios are those of star-forming gas, and we detect none of the high-ionization lines an accreting black hole would produce. Third, each companion is a compact source with its own stellar continuum, from which we derive its mass.

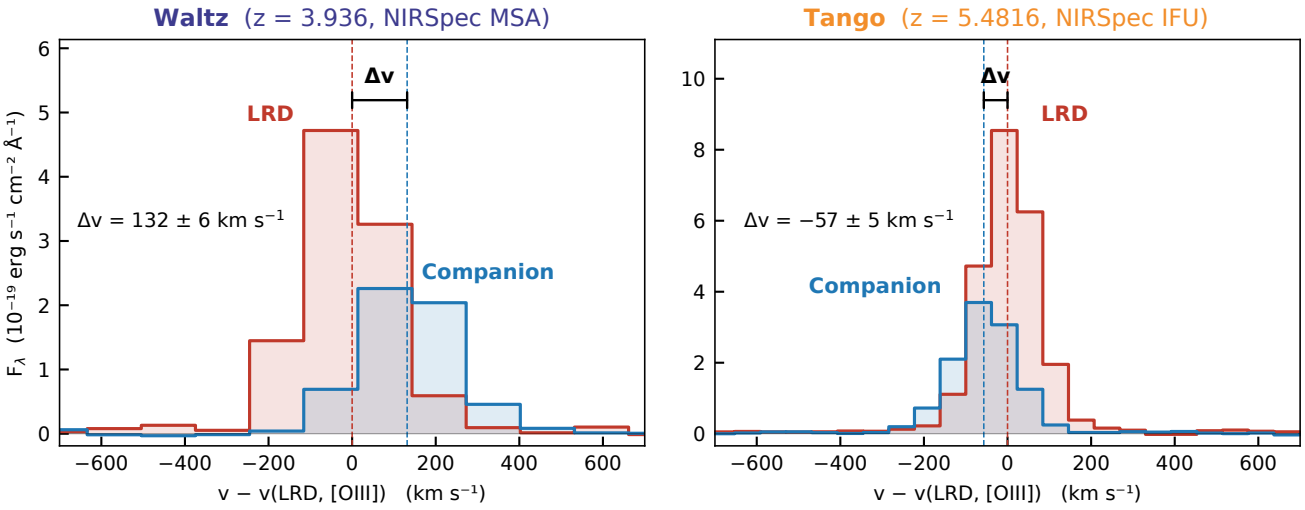


Figure 2. Velocity offsets of the two pairs. [O III]λ5008 profiles of each LRD (red) and its companion (blue), in velocity relative to the LRD centroid; dashed lines mark the two centroids. Left: Waltz, from the JADES G235M spectra, $\Delta v = +131.6 \pm 3.3\,\mathrm{km\,s^{-1}}$ (weighted mean of two independent MSA observations of the companion). Right: Tango, from the G395H cube, $\Delta v = -56.8 \pm 0.7\,\mathrm{km\,s^{-1}}$. Both offsets are line-of-sight quantities; systematic terms are included in Table 1.

In the rest-frame UV, the companions are as luminous as their LRDs. Tango's companion equals its LRD in F115W and outshines the compact nucleus alone by a factor of two; the same holds for Waltz's companion when its two knots are counted together. Each LRD therefore sits a few kpc from a source of ultraviolet radiation as bright as itself, caught within tens of Myr of a burst.

3.3. *A Black Hole in the Heavy-Seed Mass Range*

The third question concerns the LRDs themselves: how massive are their black holes, and how much have they grown since seeding? Waltz gives a cleaner answer. Its broad Hα line (Fig. 3, bottom left) is a single unabsorbed component of FWHM $1169^{+108}_{-88}\,\mathrm{km\,s^{-1}}$ required by the data at $\Delta\chi^2 = 284$. Virial calibrations bracket the mass between $\log(M_\bullet/\mathrm{M_\odot}) = 6.31$ and 6.59 (J. E. Greene & L. C. Ho 2005; A. E. Reines et al. 2013), that is, $2-4\times10^6\,\mathrm{M_\odot}$, radiating at $f_{\rm Edd} = 0.55$ with $L_{\rm bol} = 1.4\times10^{44}\,\mathrm{erg\,s^{-1}}$.

Direct collapse produces black holes of $\sim 10^4-10^6\,\mathrm{M_\odot}$ (A. Ferrara et al. 2014), so Waltz's black hole is only a factor of a few above that range. At its measured Eddington ratio, with a radiative efficiency of 0.1, one e-folding of mass takes 91 Myr, so the growth required to reach the observed mass from a heavy seed is 60 – 130 Myr at the observed rate, or longer if accretion was interrupted.

The gas around the black hole is as metal-poor and as dust-free as the companion. The narrow-line regions of both LRDs sit at the saturated maximum of the strong-line calibration, with [O III]/Hβ = 8.1 ± 1.2 in Waltz and 7.4 in Tango, and with [N II]/Hα < 0.08 and 0.008. Waltz's narrow Balmer decrement is at the Case B value, so its narrow-line gas carries no dust, while Tango's implies $A_V \simeq 0.9$ mag. Both narrow-line regions are as cold as the companions, with dispersions of ≤ 52 and $32-54\,\mathrm{km\,s^{-1}}$, and both hosts are limited to $M_\star < 8\times10^9\,\mathrm{M_\odot}$. In both systems, the red light is unresolved while the rest-UV light is extended, so we see only the host's ultraviolet.

In Waltz, a black hole of a few $10^6\,\mathrm{M_\odot}$ accretes at half the Eddington rate in metal-poor, dust-free gas, in a host with no more than a few $10^9\,\mathrm{M_\odot}$ in stars, alongside a starburst of the same gas. Every element of the environment predicted to form a heavy seed is present.

Tango hosts a more evolved black hole, but its mass is less certain. Its broad Hα (Fig. 3, bottom right) is detected at 109σ with FWHM $2132 \pm 18\,\mathrm{km\,s^{-1}}$, matched by a broad H$\beta$ of $2390 \pm 252\,\mathrm{km\,s^{-1}}$, but its core is absorbed: a single Gaussian leaves a -24σ residual within $300\,\mathrm{km\,s^{-1}}$ of the line center. With the core removed, both the width and the flux of the broad component depend on the profile assumed, leading to $\log(M_\bullet/\mathrm{M_\odot}) = 7.46-7.80$, an order of magnitude above Waltz, at $f_{\rm Edd} = 0.34$ and $L_{\rm bol} = 1.2\times10^{45}\,\mathrm{erg\,s^{-1}}$. The two systems thus sample two stages of the same growth: one black hole about one e-folding past its birth mass and one several beyond it.

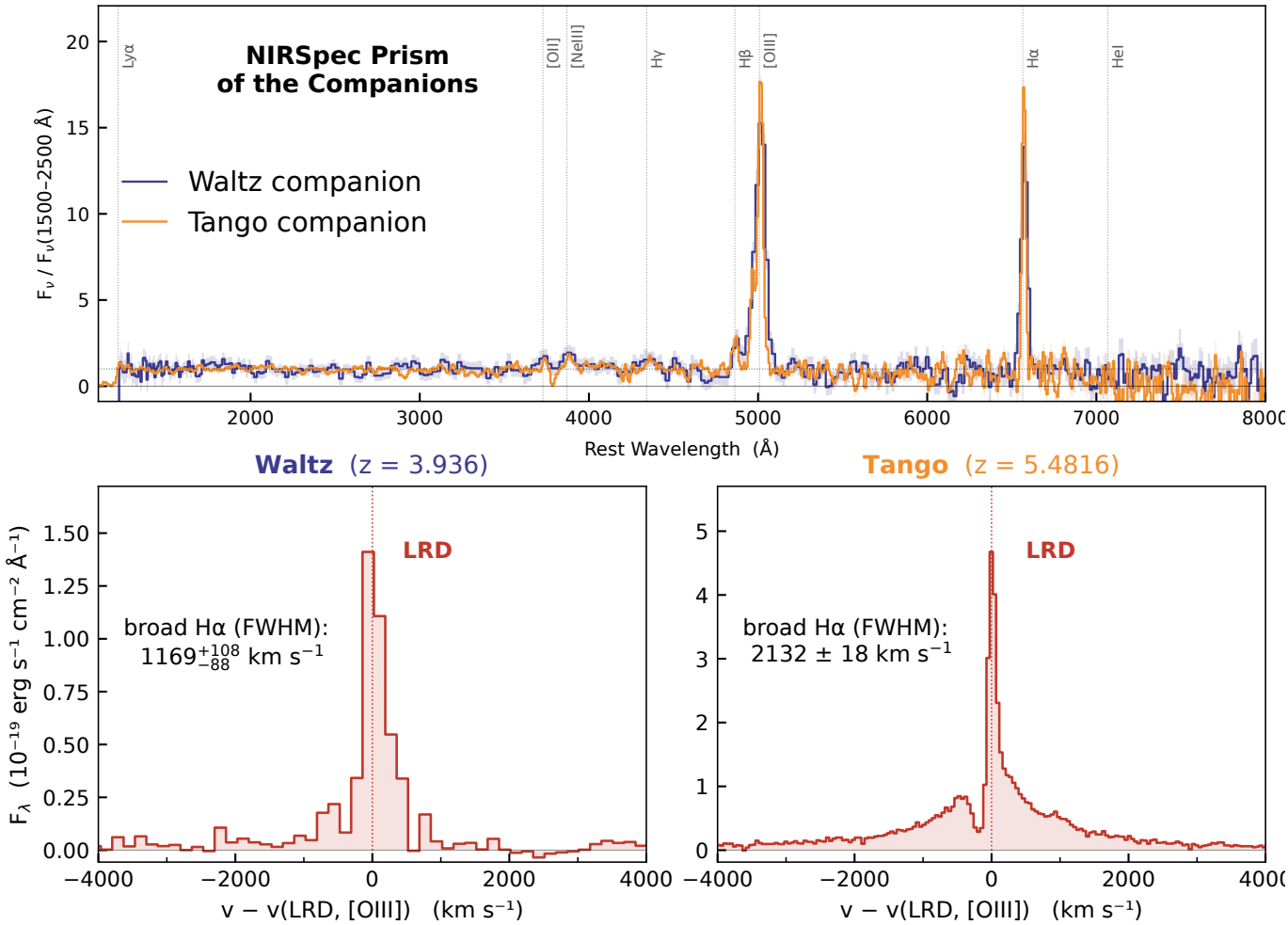


Figure 3. Spectra of the companions and of the LRDs. Top: NIRSpec prism spectra of the two companions, normalized to their mean flux density at $1500 - 2500$ Å rest-frame; shading is the 1σ uncertainty and dotted lines mark the principal transitions. The two are nearly indistinguishable across 524 Myr of cosmic time: blue continua, no measurable dust attenuation, and extreme equivalent widths, $\mathrm{EW_0(H\alpha)} = 733 \pm 80$ Å for Tango and $800 - 950$ Å for Waltz. Bottom: Hα complexes of the two LRDs, in velocity relative to their [O III] centroids. Waltz shows a clean broad line of FWHM 1169^{+108}_{-88} km s^{-1}. Tango shows a broad line of FWHM 2132 ± 18 km s^{-1} detected at 109σ, whose core is absorbed.

3.4. *Two Pairs on Their Way to a Merger*

The last question is whether the companions are bound to their LRDs, and what becomes of them. A spectroscopic pair offers two observables: (i) the projected separation and (ii) the line-of-sight velocity. As such, whether these describe a bound orbit depends on the mass between the two galaxies. Figure 4 (panel a) gives the answer as a function of the host halo mass.

For Tango, the requirement is very mild: binding needs $9.5 \times 10^8\,\mathrm{M_\odot}$ within 2.54 kpc, and the pair is bound in 81% of the realizations. For Waltz, the requirement is $7.2 \times 10^9\,\mathrm{M_\odot}$ within 3.57 kpc, so that the bound fraction is 48% over the full prior. Hence, for Waltz, the binding question turns into a dynamical measurement of an LRD host: if the pair is bound, the LRD lives in a halo of $M_{200} \gtrsim 5 \times 10^{10}\,\mathrm{M_\odot}$, with $\log(M_{200}/\,\mathrm{M_\odot}) = 10.96^{+0.38}_{-0.50}$ across the bound realizations. This is the halo at $z = 3.9$, which is about a Gyr after any heavy seed would have formed (§4). The mass must sit on the LRD's side: the companion's dispersion limits its halo to $\lesssim 10^{10}\,\mathrm{M_\odot}$, so it is the satellite in every bound orbit.

Orbital decay is dominated by dynamical friction (panel b). The median bound orbit of Tango merges in 129 Myr, i.e., before $z = 5.0$. For Waltz, it is 457 Myr, i.e., by $z \approx 3.2$. Both distributions peak well before their medians, at 22 and 231 Myr, respectively, and have long tails. Of the bound Tango orbits, 69% merge within 300 Myr and 88% within 1 Gyr; of the Waltz ones, 24% and 64%.

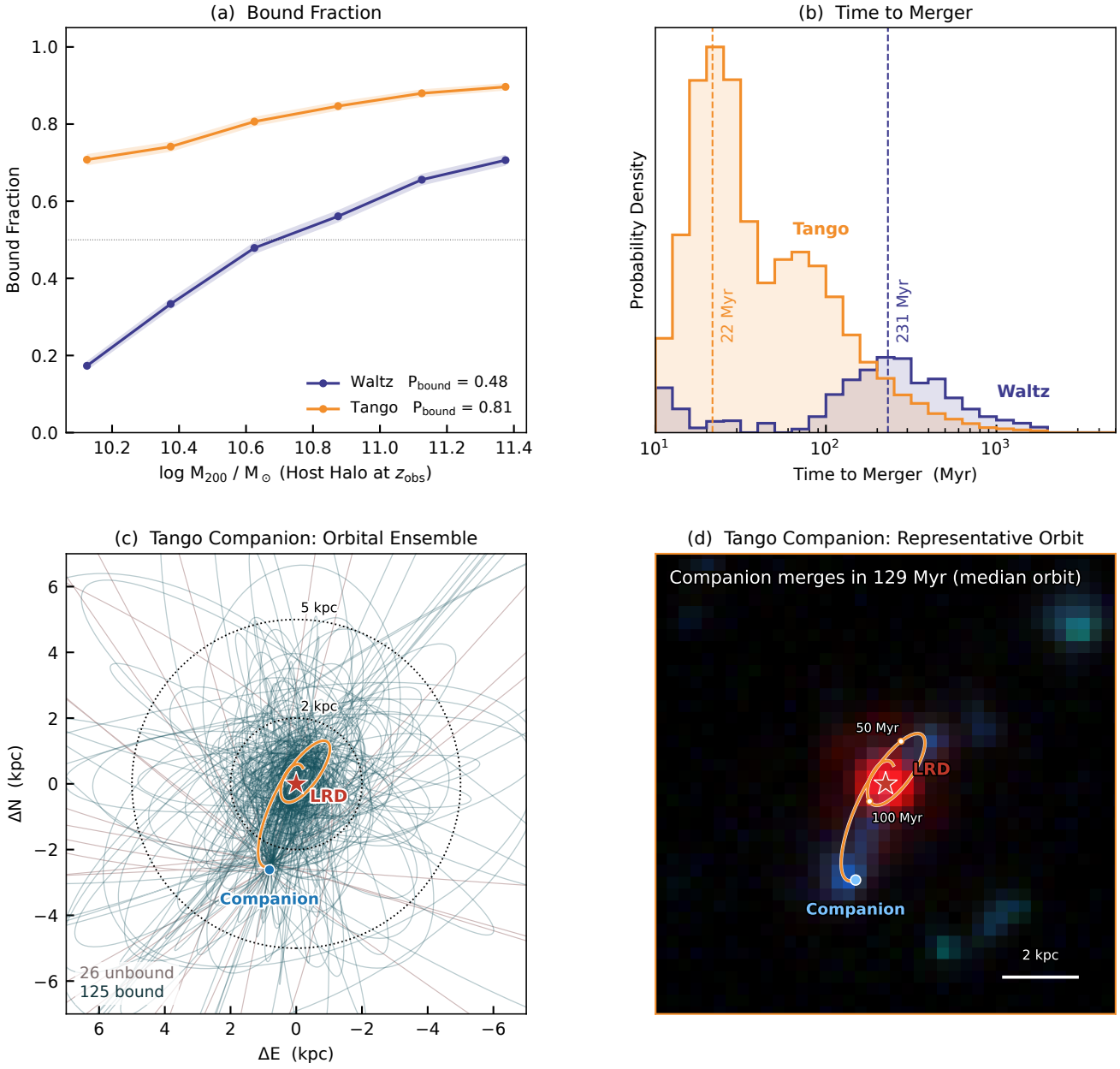


Figure 4. Orbital analysis, from Monte Carlo ensembles of 6000 orbits per system. *(a):* Fraction of bound orbits against the host halo mass: $P_{\rm bound} = 0.48$ for Waltz and 0.81 for Tango. Halo masses refer to the epoch of observation; the $\sim 10^8\,{\rm M}_\odot$ atomic-cooling halo in which a heavy seed forms at $z \gtrsim 10$ grows into this range by $z = 4-6$ (§4). *(b):* Merger-time distributions of the bound orbits. Dashed lines mark the modes, 22 Myr for Tango and 231 Myr for Waltz (medians are 129 Myr and 457 Myr, respectively). *(c):* A subset of the Tango ensemble (125 bound and 26 unbound trajectories) with the median orbit highlighted. *(d):* The median orbit, with $t_{\rm merge} = 129$ Myr, projected on the RGB composite, with marked positions after 50 and 100 Myr.

Panels c and d show what these numbers describe: a family of elongated orbits threading the LRD, with the median one implying two passages and a merger within 129 Myr. According to the median orbit, deprojected, the Tango companion is 2.95 kpc from its LRD, moving at $114\,\mathrm{km\,s^{-1}}$; the Waltz companion is 4.13 kpc away at $265\,\mathrm{km\,s^{-1}}$. Both median orbits are eccentric with circularities 0.68 and 0.49, and both pairs are within about 50 Myr of their first pericenter, at 1.24 kpc for Tango and 2.49 kpc for Waltz. In summary, we are watching the blue companion rapidly approach its LRD.

When the cosmic dance ends, the companion is inside the host of the LRD. A few $10^7 - 10^8\,\mathrm{M_\odot}$ of young, metal-poor stars and their gas arrive at black holes that are still within a few e-foldings of their birth mass. If the companion is the halo that set the collapse in motion, it ends as part of the galaxy that grows the black hole, and the LRD phase closes with a merger.

4. SUMMARY AND CONCLUSIONS

This study was motivated by observations (P. Rinaldi et al. 2025; J. F. W. Baggen et al. 2026; A. J. Barger & L. L. Cowie 2026) and a statistical analysis by F. Pacucci & C. M. Urry (2026), which found that the brightest LRDs host blue companions within 2 kpc, 2.39 times more often than matched galaxies (significant at 3.3σ), and that those companions are bluer than the companions of ordinary galaxies. That excess can be interpreted as the geometry of the "synchronized pair" (M. Dijkstra et al. 2008; E. Visbal et al. 2014; J. A. Regan et al. 2017), in which a young star-forming halo irradiates a pristine neighbor and enables the direct collapse of a heavy black hole seed. Photometry, however, left open questions that only spectroscopy can address. For example, whether (i) the companions are physical, (ii) their blue light is starlight or radiation reprocessed from the LRD, and (iii) the pairs are gravitationally bound.

This Letter presents the only two LRD–companion pairs reported in the literature with spectra of both members: Waltz, at $z = 3.936$, observed with the NIRSpec MSA, and Tango, at $z = 5.4816$, observed with the NIRSpec IFU. Our key findings are the following.

- Both companions lie at the redshift of their LRD, offset by 132 and $57\,\mathrm{km\,s^{-1}}$ at projected separations of 3.6 and 2.5 kpc.
- The two companions are identical, but separated by 524 Myr of cosmic time: starbursts $\lesssim 50$ Myr old, metal-poor ($0.2\,\mathrm{Z_\odot}$), dust-free, dynamically cold ($\sigma_{\rm int} = 20 - 65\,\mathrm{km\,s^{-1}}$), of $10^7 - 10^8\,\mathrm{M_\odot}$, and as bright as their LRDs in the rest-frame UV.
- The LRD does not power the companion's light.
- The LRD in Waltz hosts a black hole of $\approx 3 \times 10^6\,\mathrm{M_\odot}$ accreting at half the Eddington rate, only a factor of a few above the birth mass of a direct collapse black hole, inside narrow-line gas as metal-poor and dust-free as the companion, in a host of $M_\star < 8 \times 10^9\,\mathrm{M_\odot}$.
- Tango is bound in 81% of the orbital realizations; Waltz is bound if its host halo exceeds $5 \times 10^{10}\,\mathrm{M_\odot}$, so that its binding is a dynamical constraint on an LRD host. Once bound, the companions merge with their LRDs within a few hundred Myr (modes of 22 Myr for Tango and 231 Myr for Waltz).

The ages of the blue companions raise a timing question. The starbursts we observe are $\lesssim 50$ Myr old, whereas direct collapse requires gas that is (nearly) pristine (below $\sim 10^{-4} - 10^{-3}\,\mathrm{Z_\odot}$, K. Omukai et al. 2008; S. Chon & K. Omukai 2020; J. A. Regan et al. 2020). Hence, the seed must have formed before the surrounding gas was enriched: the LRDs' narrow-line regions, with [N II]/Hα < 0.08 and 0.008, are metal-poor but not pristine.

Two possibilities are open. In the standard scenario, the seed formed at $z \gtrsim 10$, and the companion is the descendant of the first halo to collapse, forming stars in episodes of which we observe the latest. In the second scenario, the whole system is young: the companions assembled most of their stars within the last ~ 100 Myr ($M_\star$/SFR ≈ 56 and 65 Myr), the Waltz black hole needs $60 - 130$ Myr to grow from a $10^6\,\mathrm{M_\odot}$ seed to its observed mass at its observed Eddington ratio, and a hundred Myr of star formation is enough to enrich the companions to the $0.2\,\mathrm{Z_\odot}$ we measure from their spectra, which is also the metallicity that galaxies of $10^7 - 10^8\,\mathrm{M_\odot}$ display at $z = 4 - 10$ (K. Nakajima et al. 2023; M. Curti et al. 2023), and for their supernova-driven winds to carry metals across the few kpc that separate them from their neighbors (M. Dijkstra et al. 2014; B. Agarwal et al. 2014).

The binding masses displayed in Fig. 4 also add an important timing argument. Direct collapse takes place in atomic-cooling halos of $\sim 10^7 - 10^8\,\mathrm{M_\odot}$ at $z \gtrsim 10$ (V. Bromm & A. Loeb 2003; K. Inayoshi et al. 2020), whereas if the Waltz pair is bound, its LRD sits in a halo of $\gtrsim 5 \times 10^{10}\,\mathrm{M_\odot}$ at $z = 3.9$. However, these two numbers refer to epochs separated by ~ 1 Gyr. Early halos on rapid growth tracks of high-σ peaks (e.g., the members of a synchronized pair) grow as $M(z) \simeq M_0\, e^{-\alpha(z-z_0)}$ with $\alpha \approx 0.8 - 1$ (A. Dekel et al. 2013; C. A. Correa et al. 2015), i.e., by a factor $e^{6\alpha} \approx 100 - 400$ between $z_0 = 10$ and $z = 4$, while

the abundance of LRDs at these redshifts independently points to hosts of this mass (F. Pacucci & A. Loeb 2025).

If the seed formed at $z \gtrsim 10$, its halo has had a billion years to grow, and we expect a mass of $5 \times 10^{10}\,M_\odot$ at $z = 3.9$. If instead the seed formed in the last $100 - 200$ Myr, its halo would have just crossed the atomic-cooling threshold, $2 - 4 \times 10^8\,M_\odot$ at $z = 4 - 6$, and could not have reached $5 \times 10^{10}\,M_\odot$ since. For Waltz, the two readings thus part ways: if the pair is bound, the seed is old; if the system is young, the pair is unbound, which its 48% bound probability allows. An old seed must then have grown slowly. Reaching $3 \times 10^6\,M_\odot$ takes $100 - 520$ Myr at the present rate for seeds of $10^6 - 10^4\,M_\odot$, against the ~ 1 Gyr elapsed since $z \approx 10$, so the black hole was active for $10 - 50\%$ of its life, as the intermittent, radiation-regulated accretion of DCBHs predicts (F. Pacucci & A. Ferrara 2015). Tango is less constraining: binding requires only $10^9\,M_\odot$ inside 2.5 kpc (Table 1), which an atomic-cooling halo alone could not supply but $\sim 10^9\,M_\odot$ of baryons in the LRD host could, so both interpretations remain open there. The young reading, where it survives, requires a near-pristine atomic-cooling halo beside a star-forming one at $z = 4 - 6$.

Such halos are expected to exist: simulations find metal-free star formation continuing in pristine pockets at the outskirts of enriched regions well past the end of reionization (L. Tornatore et al. 2007; M. Trenti et al. 2009; B. Liu & V. Bromm 2020; A. Venditti et al. 2026), with the sites shifting to atomic-cooling halos by $z \sim 5$ (S. Hegde & S. R. Furlanetto 2025). In addition, Population III candidates are now reported at $z = 6 - 8$ (E. Vanzella et al. 2023; S. Fujimoto et al. 2025). Of course, our observations cannot establish whether such a pocket existed next to the companion at the time of collapse.

Whichever the timing, the end is the same. Within a few hundred Myr, the companion falls into the LRD with its stars: $\sim 10^8\,M_\odot$ of young, metal-poor stars. The LRD hosts are faint and unresolved in the rest-frame optical, with only upper limits on stellar masses, so the merger adds a stellar component of $\sim 10^8\,M_\odot$ to a host of small stellar mass, around a black hole that is already $10^6 - 10^7\,M_\odot$. Thus, the synchronized pair mechanism first generates the seed, then forms the seed's first galaxy. A black hole that acquires its stars after forming is overmassive by definition, and it descends toward the local relation only as the host assembles around it. The LRD phase may be the moment between the two acts, when the black hole is there while its galaxy is still inbound.

If such infalls recur, the LRD phase has a natural clock. Each one adds $\sim 10^8\,M_\odot$ of stars within a few hundred Myr. Over a Gyr, several would add $\sim 10^9\,M_\odot$ of stars to the LRD host, along with gas to fuel in situ star formation. The accreted stars alone are not enough to carry a 10^6–$10^7\,M_\odot$ black hole onto the local relation, but the sequence of infalls could end the phase in which the dot outshines its galaxy, on the same Gyr timescale over which LRDs disappear below $z \approx 4$ (e.g., D. D. Kocevski et al. 2025; V. Kokorev et al. 2024; F. Pacucci & A. Loeb 2025).

Although based only on two systems, our study highlights the urgent need to investigate LRDs' immediate surroundings, which have received relatively little attention to date, with only a handful of often shallow spectroscopic observations.

In summary, spectroscopy of LRDs' blue companions shows they are real, young, metal-poor starbursts falling in. With Waltz and Tango, we are watching two steps of the same dance at two epochs: a heavy black hole seed beside the galaxy that may have lit its collapse, a few hundred Myr before the two become one.

ACKNOWLEDGMENTS

F.P. acknowledges support from NASA through Chandra Award No. GO3-24087A and JWST Award No. JWST-GO-03805.010-A. P.R. acknowledges support from the University of Texas at Austin Cosmic Frontier Center. Some of the data products presented herein were retrieved from the Dawn JWST Archive (DJA), an initiative of the Cosmic Dawn Center, funded under grant DNRF140.

Software: astropy (Astropy Collaboration et al. 2022), numpy (C. R. Harris et al. 2020), scipy (P. Virtanen et al. 2020), matplotlib (J. D. Hunter 2007), EAZY (G. B. Brammer et al. 2008), SEP (K. Barbary 2016), bagpipes (A. C. Carnall et al. 2019), grizli (G. Brammer 2023)

REFERENCES

Agarwal, B., Dalla Vecchia, C., Johnson, J. L., Khochfar, S., & Paardekooper, J.-P. 2014, MNRAS, 443, 648, doi: 10.1093/mnras/stu1112

Akins, H. B., Casey, C. M., Lambrides, E., et al. 2025, ApJ, 991, 37, doi: 10.3847/1538-4357/ade984

Astropy Collaboration, Price-Whelan, A. M., Lim, P. L., et al. 2022, ApJ, 935, 167, doi: 10.3847/1538-4357/ac7c74

Baggen, J. F. W., Scoggins, M. T., van Dokkum, P., et al. 2026, ApJL, 1002, L4, doi: 10.3847/2041-8213/ae58a5

Baggen, J. F. W., van Dokkum, P., Labbé, I., et al. 2023, ApJL, 955, L12, doi: 10.3847/2041-8213/acf5ef

Barbary, K. 2016, The Journal of Open Source Software, 1, 58, doi: 10.21105/joss.00058

Barger, A. J., & Cowie, L. L. 2026, arXiv e-prints, arXiv:2605.27903. https://arxiv.org/abs/2605.27903

Begelman, M. C., Volonteri, M., & Rees, M. J. 2006, MNRAS, 370, 289, doi: 10.1111/j.1365-2966.2006.10467.x

Bellovary, J. 2025, ApJL, 984, L55, doi: 10.3847/2041-8213/adce6c

Brammer, G. 2023, grizli, 1.9.11 Zenodo, doi: 10.5281/zenodo.8370018

Brammer, G. B., van Dokkum, P. G., & Coppi, P. 2008, ApJ, 686, 1503, doi: 10.1086/591786

Bromm, V., & Loeb, A. 2003, ApJ, 596, 34, doi: 10.1086/377529

Bruzual, G., & Charlot, S. 2003, MNRAS, 344, 1000, doi: 10.1046/j.1365-8711.2003.06897.x

Carnall, A. C., McLure, R. J., Dunlop, J. S., et al. 2019, MNRAS, 490, 417, doi: 10.1093/mnras/stz2544

Chabrier, G. 2003, PASP, 115, 763, doi: 10.1086/376392

Chandrasekhar, S. 1943, ApJ, 97, 255, doi: 10.1086/144517

Chen, C.-H., Ho, L. C., Li, R., & Inayoshi, K. 2025a, ApJL, 989, L12, doi: 10.3847/2041-8213/adee0a

Chen, C.-H., Ho, L. C., Li, R., & Zhuang, M.-Y. 2025b, ApJ, 983, 60, doi: 10.3847/1538-4357/ada93a

Chisholm, J., Berg, D. A., Boylan-Kolchin, M., et al. 2026, ApJL, 1004, L4, doi: 10.3847/2041-8213/ae6dae

Chon, S., & Omukai, K. 2020, MNRAS, 494, 2851, doi: 10.1093/mnras/staa863

Correa, C. A., Wyithe, J. S. B., Schaye, J., & Duffy, A. R. 2015, MNRAS, 450, 1514, doi: 10.1093/mnras/stv689

Curti, M., Mannucci, F., Cresci, G., & Maiolino, R. 2020, MNRAS, 491, 944, doi: 10.1093/mnras/stz2910

Curti, M., D'Eugenio, F., Carniani, S., et al. 2023, MNRAS, 518, 425, doi: 10.1093/mnras/stac2737

Decarli, R., Loiacono, F., Farina, E. P., et al. 2024, A&A, 689, A219, doi: 10.1051/0004-6361/202449239

Dekel, A., Zolotov, A., Tweed, D., et al. 2013, MNRAS, 435, 999, doi: 10.1093/mnras/stt1338

D'Eugenio, F., Nelson, E., Ji, X., et al. 2025a, arXiv e-prints, arXiv:2510.00101, doi: 10.48550/arXiv.2510.00101

D'Eugenio, F., Cameron, A. J., Scholtz, J., et al. 2025b, ApJS, 277, 4, doi: 10.3847/1538-4365/ada148

Dijkstra, M., Ferrara, A., & Mesinger, A. 2014, MNRAS, 442, 2036, doi: 10.1093/mnras/stu1007

Dijkstra, M., Haiman, Z., Mesinger, A., & Wyithe, J. S. B. 2008, MNRAS, 391, 1961, doi: 10.1111/j.1365-2966.2008.14031.x

Draine, B. T., & Bertoldi, F. 1996, ApJ, 468, 269, doi: 10.1086/177689

Durodola, E., Pacucci, F., & Hickox, R. C. 2025, ApJ, 985, 169, doi: 10.3847/1538-4357/adced2

Eisenstein, D. J., Willott, C., Alberts, S., et al. 2026, ApJS, 283, 6, doi: 10.3847/1538-4365/ae3163

Eldridge, J. J., Stanway, E. R., Xiao, L., et al. 2017, PASA, 34, e058, doi: 10.1017/pasa.2017.51

Ferrara, A., Salvadori, S., Yue, B., & Schleicher, D. 2014, MNRAS, 443, 2410, doi: 10.1093/mnras/stu1280

Fujimoto, S., Naidu, R. P., Chisholm, J., et al. 2025, ApJ, 989, 46, doi: 10.3847/1538-4357/ade9a1

Golubchik, M., Furtak, L. J., Allingham, J. F. V., et al. 2026, A&A, 710, A226, doi: 10.1051/0004-6361/202558407

Greene, J. E., & Ho, L. C. 2005, ApJ, 630, 122, doi: 10.1086/431897

Greene, J. E., Labbe, I., Goulding, A. D., et al. 2024, ApJ, 964, 39, doi: 10.3847/1538-4357/ad1e5f

Gunasekera, C. M., van Hoof, P. A. M., Dehghanian, M., et al. 2025, RMxAA, 61, 120, doi: 10.22201/ia.01851101p.2025.61.03.01

Gupta, A. R., Taylor, A., Curtis-Lake, E., et al. 2026, arXiv e-prints, arXiv:2605.30414, doi: 10.48550/arXiv.2605.30414

Harikane, Y., Zhang, Y., Nakajima, K., et al. 2023, ApJ, 959, 39, doi: 10.3847/1538-4357/ad029e

Harris, C. R., Millman, K. J., van der Walt, S. J., et al. 2020, Nature, 585, 357, doi: 10.1038/s41586-020-2649-2

Hegde, S., & Furlanetto, S. R. 2025, The Open Journal of Astrophysics, 8, 147, doi: 10.33232/001c.145070

Helton, J. M., Sun, F., Woodrum, C., et al. 2024, ApJ, 974, 41, doi: 10.3847/1538-4357/ad6867

Hernquist, L. 1990, ApJ, 356, 359, doi: 10.1086/168845

Hunter, J. D. 2007, Computing in Science and Engineering, 9, 90, doi: 10.1109/MCSE.2007.55

Husemann, B., Wisotzki, L., Sánchez, S. F., & Jahnke, K. 2013, A&A, 549, A43, doi: 10.1051/0004-6361/201220076

Hviding, R. E., de Graaff, A., Liu, H., et al. 2026, ApJL, 1000, L18, doi: 10.3847/2041-8213/ae4c88

Inayoshi, K., Visbal, E., & Haiman, Z. 2020, ARA&A, 58, 27, doi: 10.1146/annurev-astro-120419-014455

Ishikawa, Y., Eilers, A.-C., Naidu, R. P., et al. 2026a, arXiv e-prints, arXiv:2607.09647, doi: 10.48550/arXiv.2607.09647

Jakobsen, P., Ferruit, P., Alves de Oliveira, C., et al. 2022, A&A, 661, A80, doi: 10.1051/0004-6361/202142663
Jones, B. L., Kocevski, D. D., Pacucci, F., et al. 2025, arXiv e-prints, arXiv:2510.07376, doi: 10.48550/arXiv.2510.07376
Juodžbalis, I., Ji, X., D'Eugenio, F., et al. 2026, arXiv e-prints, arXiv:2607.19057, doi: 10.48550/arXiv.2607.19057
Killi, M., Watson, D., Brammer, G., et al. 2024, A&A, 691, A52, doi: 10.1051/0004-6361/202348857
Kocevski, D. D., Onoue, M., Inayoshi, K., et al. 2023, ApJL, 954, L4, doi: 10.3847/2041-8213/ace5a0
Kocevski, D. D., Finkelstein, S. L., Barro, G., et al. 2025, ApJ, 986, 126, doi: 10.3847/1538-4357/adbc7d
Kokorev, V., Caputi, K. I., Greene, J. E., et al. 2024, ApJ, 968, 38, doi: 10.3847/1538-4357/ad4265
Korhonen Cuestas, N. A., Strom, A. L., Miller, T. B., et al. 2025, ApJ, 984, 188, doi: 10.3847/1538-4357/adc5f7
Lambrides, E., Larson, R. L., Garofali, K., et al. 2026, Nature Astronomy, 10, 868, doi: 10.1038/s41550-026-02813-w
Latif, M. A., Bovino, S., Van Borm, C., et al. 2014, MNRAS, 443, 1979, doi: 10.1093/mnras/stu1230
Leitherer, C., Schaerer, D., Goldader, J. D., et al. 1999, ApJS, 123, 3, doi: 10.1086/313233
Leja, J., Carnall, A. C., Johnson, B. D., Conroy, C., & Speagle, J. S. 2019, ApJ, 876, 3, doi: 10.3847/1538-4357/ab133c
Liu, B., & Bromm, V. 2020, MNRAS, 497, 2839, doi: 10.1093/mnras/staa2143
Lodato, G., & Natarajan, P. 2006, MNRAS, 371, 1813, doi: 10.1111/j.1365-2966.2006.10801.x
Loeb, A., & Rasio, F. A. 1994, ApJ, 432, 52, doi: 10.1086/174548
Madau, P., & Haardt, F. 2024, ApJL, 976, L24, doi: 10.3847/2041-8213/ad90e1
Maiolino, R., Scholtz, J., Curtis-Lake, E., et al. 2024, A&A, 691, A145, doi: 10.1051/0004-6361/202347640
Maiolino, R., Risaliti, G., Signorini, M., et al. 2025, MNRAS, 538, 1921, doi: 10.1093/mnras/staf359
Marshall, M. A., Perna, M., Willott, C. J., et al. 2023, A&A, 678, A191, doi: 10.1051/0004-6361/202346113
Matthee, J., Naidu, R. P., Brammer, G., et al. 2024, ApJ, 963, 129, doi: 10.3847/1538-4357/ad2345
Matthee, J., Torralba, A., Pezzulli, G., et al. 2026, arXiv e-prints, arXiv:2603.17667, doi: 10.48550/arXiv.2603.17667
Modelevsky, E., Nitzan, O., Sari, R., & Quataert, E. 2026, arXiv e-prints, arXiv:2608.05283. https://arxiv.org/abs/2608.05283
Naidu, R. P., Matthee, J., Katz, H., et al. 2026, Nature, 656, 329, doi: 10.1038/s41586-026-10846-4
Nakajima, K., Ouchi, M., Isobe, Y., et al. 2023, ApJS, 269, 33, doi: 10.3847/1538-4365/acd556
Nandal, D., & Loeb, A. 2026, ApJ, 998, 124, doi: 10.3847/1538-4357/ae32f3
Navarro, J. F., Frenk, C. S., & White, S. D. M. 1996, ApJ, 462, 563, doi: 10.1086/177173
Navarro-Carrera, R., Rinaldi, P., Caputi, K. I., et al. 2026, ApJ, 996, 70, doi: 10.3847/1538-4357/ae1609
Oh, S. P., & Haiman, Z. 2002, ApJ, 569, 558, doi: 10.1086/339393
Omukai, K. 2001, ApJ, 546, 635, doi: 10.1086/318296
Omukai, K., Schneider, R., & Haiman, Z. 2008, ApJ, 686, 801, doi: 10.1086/591636
Osterbrock, D. E., & Ferland, G. J. 2006, Astrophysics of gaseous nebulae and active galactic nuclei (University Science Books)
Pacucci, F., & Ferrara, A. 2015, MNRAS, 448, 104, doi: 10.1093/mnras/stv018
Pacucci, F., Ferrara, A., & Kocevski, D. D. 2026, arXiv e-prints, arXiv:2601.14368, doi: 10.48550/arXiv.2601.14368
Pacucci, F., & Loeb, A. 2025, ApJL, 989, L19, doi: 10.3847/2041-8213/ade871
Pacucci, F., & Narayan, R. 2024, ApJ, 976, 96, doi: 10.3847/1538-4357/ad84f7
Pacucci, F., Nguyen, B., Carniani, S., Maiolino, R., & Fan, X. 2023, ApJL, 957, L3, doi: 10.3847/2041-8213/ad0158
Pacucci, F., & Urry, C. M. 2026, ApJL, 1010, L2, doi: 10.3847/2041-8213/aeaa52
Pérez-González, P. G., Barro, G., Carniani, S., et al. 2026, arXiv e-prints, arXiv:2602.20247, doi: 10.48550/arXiv.2602.20247
Planck Collaboration, Aghanim, N., Akrami, Y., et al. 2020, A&A, 641, A6, doi: 10.1051/0004-6361/201833910
Regan, J. A., Haiman, Z., Wise, J. H., O'Shea, B. W., & Norman, M. L. 2020, The Open Journal of Astrophysics, 3, E9, doi: 10.21105/astro.2006.14625
Regan, J. A., Visbal, E., Wise, J. H., et al. 2017, Nature Astronomy, 1, 0075, doi: 10.1038/s41550-017-0075
Reines, A. E., Greene, J. E., & Geha, M. 2013, ApJ, 775, 116, doi: 10.1088/0004-637X/775/2/116
Rieke, M. J., Robertson, B., Tacchella, S., et al. 2023a, ApJS, 269, 16, doi: 10.3847/1538-4365/acf44d
Rieke, M. J., Kelly, D. M., Misselt, K., et al. 2023b, PASP, 135, 028001, doi: 10.1088/1538-3873/acac53
Rinaldi, P., Bonaventura, N., Rieke, G. H., et al. 2025, ApJ, 992, 71, doi: 10.3847/1538-4357/adfa10

Rinaldi, P., Hainline, K., D'Eugenio, F., et al. 2026a, arXiv e-prints, arXiv:2604.07138, doi: 10.48550/arXiv.2604.07138

Rinaldi, P., Rieke, G. H., Wu, Z., et al. 2026b, ApJ, 1006, 205, doi: 10.3847/1538-4357/ae80cd

Rusakov, V., Watson, D., Nikopoulos, G. P., et al. 2026, Nature, 649, 574, doi: 10.1038/s41586-025-09900-4

Setton, D. J., Greene, J. E., de Graaff, A., et al. 2025, ApJ, 995, 118, doi: 10.3847/1538-4357/ae1500

Taylor, A. J., Finkelstein, S. L., Kocevski, D. D., et al. 2025, ApJ, 986, 165, doi: 10.3847/1538-4357/add15b

Theios, R. L., Steidel, C. C., Strom, A. L., et al. 2019, ApJ, 871, 128, doi: 10.3847/1538-4357/aaf386

Tornatore, L., Ferrara, A., & Schneider, R. 2007, MNRAS, 382, 945, doi: 10.1111/j.1365-2966.2007.12215.x

Trenti, M., Stiavelli, M., & Shull, J. M. 2009, ApJ, 700, 1672, doi: 10.1088/0004-637X/700/2/1672

Valentino, F., Brammer, G., Gould, K. M. L., et al. 2023, ApJ, 947, 20, doi: 10.3847/1538-4357/acbefa

Vanzella, E., Loiacono, F., Bergamini, P., et al. 2023, A&A, 678, A173, doi: 10.1051/0004-6361/202346981

Venditti, A., Schaerer, D., Zackrisson, E., et al. 2026, The Open Journal of Astrophysics, 9, 67811, doi: 10.33232/001c.167811

Ventou, E., Contini, T., Bouché, N., et al. 2017, A&A, 608, A9, doi: 10.1051/0004-6361/201731586

Virtanen, P., Gommers, R., Oliphant, T. E., et al. 2020, Nature Methods, 17, 261, doi: 10.1038/s41592-019-0686-2

Visbal, E., Haiman, Z., & Bryan, G. L. 2014, MNRAS, 445, 1056, doi: 10.1093/mnras/stu1794